*RMxAC*, **58**, 45–47 (2024)

# THE DECAM MAGELLANIC CLOUDS EMISSION-LINE SURVEYS

S. D. Points[1], K. S. Long[2,3], W. P. Blair[4], P. F. Winkler[5], R. M. Williams[6], and Y.-H. Chu[7]

RESUMEN

Hemos utilizado la Cámara de Energía Oscura (DECam) en el telescopio CTIO Blanco de 4 metros para realizar un nuevo estudio de líneas de emisión de las Nubes Grande y Pequeña de Magallanes (LMC y SMC, respectivamente) con una resolución espacial sin precedentes, utilizando filtros H$\alpha$ de banda estrecha y [S,II], además de una banda de continuo para sustracción. Estos datos son comparables en profundidad a los estudios de líneas de emisión existentes de las Nubes de Magallanes (por ejemplo, MCELS), pero con una mayor resolución angular. Hemos creado una pipeline personalizada basada en Python para reducir estos datos y presentar ejemplos de nuestros primeros resultados.

ABSTRACT

We have used the Dark Energy Camera (DECam) on the CTIO Blanco 4-m telescope to perform a new emission-line survey of the Large and Small Magellanic Clouds (LMC and SMC, respectively) with unprecedented spatial resolution, using narrow-band H$\alpha$ and [S II] filters in addition to a continuum band for use in subtraction. These data are comparable in depth to extant emission-line surveys of the Magellanic Clouds (e.g., MCELS), but with higher angular resolution. We have created a custom Python-based pipeline to reduce these data and present examples of our first results.

*Key Words:* H II regions — ISM: supernova remnants — Magellanic Clouds

## 1. INTRODUCTION

The Large and Small Magellanic Clouds (LMC & SMC) are the two most significant satellite galaxies of the Milky Way, at distances of 50 and 60 kpc (Pietrzyński et al. 2019; Graczyk et al. 2020), and experience low galactic foreground extinction. They are the best laboratories to investigate a wide variety of astrophysical phenomena, including the life cycle of stars and the interplay between stars and the interstellar medium (ISM).

High-quality optical emission line imagery is key for such investigations, showing both the morphology and ionization structure of nebular emission on all scales and permitting meaningful comparisons with multi-wavelength data sets. For the Magellanic Clouds (MCs), the most widely used optical survey has been the Magellanic Cloud Emission-Line Survey (MCELS, Smith & MCELS Team 1999), which provided imagery with $\sim5''$ resolution. Recently, higher resolution emission-line data for much of the MCs has been obtained with the Dark Energy Camera (DECam, Honscheid & DePoy 2008; Flaugher et al. 2015) on the CTIO Blanco 4 m telescope.

In §2, we describe the DECam observations of the MCs. We discuss the data reduction in §3 and preset our results in §4. We summarize our work in §5.

## 2. OBSERVATIONS

The DECam images were obtained using the N662 (H$\alpha$ + [N II]$\lambda\lambda6548, 6583$) and N673 ([S II]$\lambda\lambda6716, 6731$) filters in addition to the DES $r'$ for continuum-subtraction. The narrow band filters are hereafter referred to as the H$\alpha$ and [S II] filters. DECam is a wide-field CCD imager with 62 science detectors that images 3 square degrees (2.2° wide) at $0.263''$ resolution (although the images are seeing limited).

The inner 54 deg$^2$ of the LMC was covered by 20 DECam fields and the inner 18.2 deg$^2$ of the SMC was covered by 5 DECam fields. Each field was observed with short and long exposures, with dithers between each exposure to fill in the detector gaps.

[1]NSF's NOIRLab, CTIO, Casilla 603, La Serena, Chile.

[2]Space Telescope Science Institute, 3700 San Martin Dr, Baltimore MD, 21218, USA.

[3]Eureka Scientific, Inc.,2452 Delmer Street, Suite 100, Oakland, CA 94602-3017, USA.

[4]The William H. Miller III Department of Physics and Astronomy, Johns Hopkins University, 3400 N. Charles Street, Baltimore, MD, 21218, USA.

[5]Department of Physics, Middlebury College, Middlebury, VT, 05753, USA.

[6]Department of Earth and Space Sciences, Columbus State University, 4225 University Avenue, Columbus, Georgia 31907, USA.

[7]Academia Sinica, 11F of AS/NTU Astronomy-Mathematics Building, No.1, Sec. 4, Roosevelt Rd, Taipei 10617, Taiwan, R.O.C.

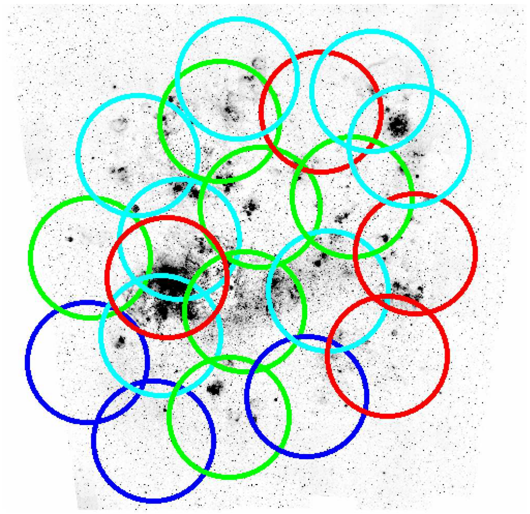

Fig. 1. MCELS Hα mosaic of the LMC with 2° diameter circles representing the approximate DECam footprint overlaid for all narrow band data. The colors of the circles represent the completeness of the long observations compared to the desired uniform depth: $\geq 2/3$ complete in Hα and [S II] (green); $\geq 2/3$ complete in Hα and $\leq 2/3$ complete in [S II] (blue); $\leq 2/3$ complete in Hα and $\geq 2/3$ complete in [S II] (cyan); and $\leq 2/3$ complete in both Hα and [S II] (red).

For the long exposures, a total of $6 \times 800$s were obtained in Hα and $12 \times 800$s in [S II][8]. We present the MCELS Hα images of the LMC and SMC with the DECam fields marked in Fig. 1 and 2, respectively.

## 3. DATA REDUCTION

The data contained in the survey were obtained over a number of nights and under varying conditions. Our goal in reducing these data was to produce moasicked versions of these images and to accurately represent diffuse emission (on large and small scales) at brightness levels that are significantly lower than those observed from the night sky. This is further complicated because the broad band $r'$ filter contains emission from both Hα and [S II], making continuum-subtraction difficult.

To reduce these data, we begin with data processed by the DECam Community Pipeline (DCP, Valdes et al. 2014). After a data quality assessment to remove observations with seeing values $\geq 1.5''$, we used custom Python-based programs[9] that make extensive use of SWarp (Bertin et al. 2002) to produce our final continuum-subtracted images. The primary steps of the KRED package are described below:

- Re-scale all data to a common magnitude scale to facilitate image subtraction and remove a single backkground value from all CCDs.
- Create a $4 \times 4$ grid of overlapping tiles for each field as a convenience to allow for producing uniform data products.
- Sort the observations by exposure times and filters and measure the difference in flux levels of overlapping detectors. These differences are used place exposures of a given exposure time and filter a common background level.
- Use SWarp to combine images in each filter based on exposure time to place the stacked images on a common world coordinate system.
- Create a "line-free" continuum image using data from all observations and subtract these continuum images from the emission-line images.

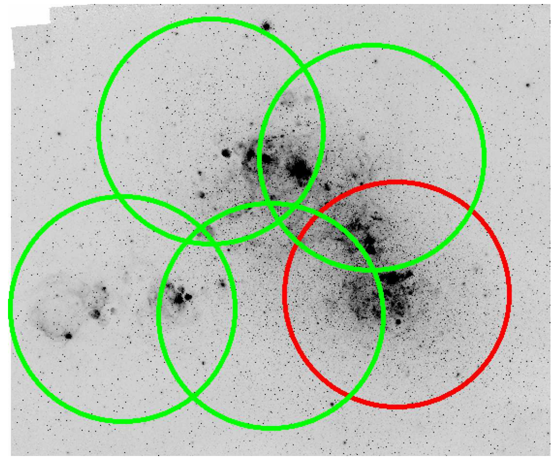

Fig. 2. MCELS Hα mosaic of the SMC with the same labeling scheme as Fig 1.

## 4. RESULTS

Although we consider the currently available data products to be preliminary, the superior resolution and overall depth and quality of the DECam images is apparent. Below we show examples of these data toward different types of interstellar structures and compare them to the MCELS data.

### 4.1. *Small H II Regions*

Isolated massive stars produce small H II regions through their ionizing radiation and wind-blown

[8]As shown in Fig. 1 and 2, neither the LMC nor the SMC were completely covered to the desired extent and depth by our observations. Some fields were either missed, under-observed, or affected by poor seeing, creating significant 'holes' in the survey data

[9]The current version of the reduction pipeline, referred to as KRED, can be found on github at `https://github.com/kslong/kred`. We would be pleased to have others make use of it, and/or to help improve it further.

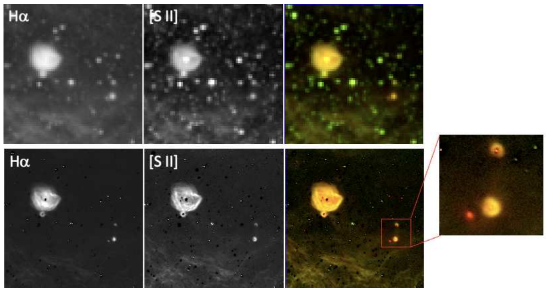


Fig. 3. A comparison of MCELS and DECam data for a small region from a field that contains several small to very small star forming regions. The top row shows MCELS H$\alpha$ and [S II] images in black and white with a color combination at right (red: H$\alpha$; green: [S II]). Yellow indicates that both ions are strong. The bottom row shows the same sequence, but for our DECam data. For scale, the box at right is 30″. These small emission nebulae are completely unresolved in the MCELS data.

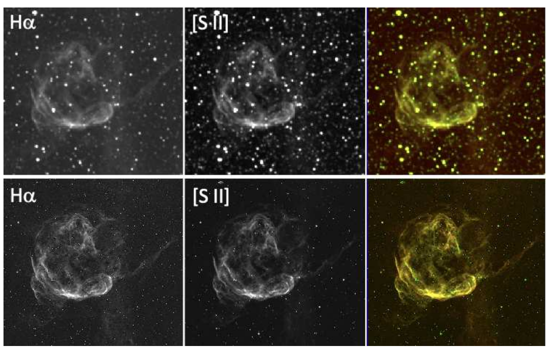


Fig. 4. A comparison of MCELS and DECam data for the faint SNR 0527−6549. Presentation is the same as in Fig. 3. This is a low surface brightness SNR. For scale, the SNR is about 250″ in diameter.

bubbles through the action of their stellar winds. As shown in Fig. 3, these small nebulae are unresolved in MCELS, but are readily apparent in our DECam data.

### 4.2. *Supernova Remnants (SNRs)*

One of the main science goals of the DECam survey was to obtain higher resolution images of the known SNR population and to search for fainter, larger, and presumably older SNRs that are beginning to merge back into the ISM (cf, Yew et al. 2021). Fig. 4 shows a comparison between the MCELS and DECam data for a faint, isolated SNR in the LMC. Williams et al. (2024, this volume) discuss the MC SNR population as seen by DECam in more detail.

### 4.3. *Bubbles and Superbubbles*

Fig. 5 shows the region surrounding N70 (Henize 1956), an isolated nebular superbubble in the eastern

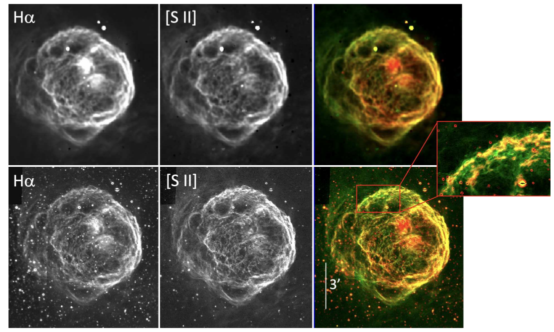


Fig. 5. A comparison of MCELS and DECam data for the N 70, a superbubble ∼7.8′ in diameter and located in an isolated region in the eastern LMC. The presentation is the same as Fig 3 and the scale is shown in the lower right color panel. The inset at right shows detail of the northern rim.

LMC, also known as DEM L301 (Davies et al. 1976). N70 has a diameter of 7.8′ (∼105 pc) and surrounds the stellar association LH 114 (Lucke & Hodge 1970).

## 5. SUMMARY

We have conducted a recent H$\alpha$ and [S II] emission-line survey of the MCs using DECam. The data have been reduced using our pipeline to produce a uniform set of flux-calibrated, continuum-subtracted images that show a remarkable improvement in angular resolution when compared to the MCELS survey. These data will enable a broad-range of ISM science and provide a legacy resource for many future research programs.

## REFERENCES

Bertin, E., Mellier, Y., Radovich, M., et al. 2002, Astronomical Data Analysis Software and Systems XI, 281, 228

Davies, R. D., Elliott, K. H., & Meaburn, J. 1976, MmRAS, 81, 89

Flaugher, B., Diehl, H. T., Honscheid, K., et al. 2015, AJ, 150, 150. doi:10.1088/0004-6256/150/5/150

Graczyk, D., Pietrzyński, G., Thompson, I. B., et al. 2020, ApJ, 904, 13. doi:10.3847/1538-4357/abbb2b

Henize, K. G. 1956, ApJS, 2, 315. doi:10.1086/190025

Honscheid, K. & DePoy, D. L. 2008, arXiv:0810.3600. doi:10.48550/arXiv.0810.3600

Lucke, P. B. & Hodge, P. W. 1970, AJ, 75, 171. doi:10.1086/110959

Pietrzyński, G., Graczyk, D., Gallenne, A., et al. 2019, Nature, 567, 200. doi:10.1038/s41586-019-0999-4

Smith, R. C. & MCELS Team 1999, New Views of the Magellanic Clouds, 190, 28

Valdes, F., Gruendl, R., & DES Project 2014, Astronomical Data Analysis Software and Systems XXIII, 485, 379

Yew, M., Filipović, M. D., Stupar, M., et al. 2021, MNRAS, 500, 2336. doi:10.1093/mnras/staa3382